ML–ResNet: a novel network to detect and locate myocardial infarction using 12 leads ECG

Chuang Han , Li Shi

PII: S0169-2607(19)30899-5
DOI: https://doi.org/10.1016/j.cmpb.2019.105138
Reference: COMM 105138

To appear in: *Computer Methods and Programs in Biomedicine*

Received date: 10 June 2019
Revised date: 13 October 2019
Accepted date: 15 October 2019

Please cite this article as: Chuang Han , Li Shi , ML–ResNet: a novel network to detect and locate myocardial infarction using 12 leads ECG, *Computer Methods and Programs in Biomedicine* (2019), doi: https://doi.org/10.1016/j.cmpb.2019.105138

Highlights

- A novel ML–ResNet model combining a single lead feature branch network with three residual blocks and feature fusion method is employed to detect and locate MI via 12 leads ECG records.
- The single lead feature branch network can learn the representative features of different levels between different layers, which exploits local characteristics of ECG to characterize the spatial information representation.
- Two schemes including intra-patient scheme and inter-patient scheme, are both performed, displaying more vital clinical significance.
- Compared with published literatures, the proposed model for MI detection and location has achieved the best results.

ML–ResNet: a novel network to detect and locate myocardial infarction using 12 leads ECG

Chuang Han[a], Li Shi[a,b,c,*]

[a] School of electrical engineering, Zhengzhou university, Zhengzhou City, Henan, China

[b] Department of automation, Tsinghua university, Beijing City, Beijing, China

[c] Beijing National Research Center For Information Science And Technology, Beijing City, Beijing, China

Abstract:

Background and Objective: Myocardial infarction (MI) is one of the most threatening cardiovascular diseases for human beings, which can be diagnosed by electrocardiogram (ECG). Automated detection methods based on ECG focus on extracting handcrafted features. However, limited by the performance of traditional methods and individual differences between patients, it's difficult for predesigned features to detect MI with high performance.

Methods: The paper presents a novel method to detect and locate MI combining a multi-lead residual neural network (ML–ResNet) structure with three residual blocks and feature fusion via 12 leads ECG records. Specifically, single lead feature branch network is trained to automatically learn the representative features of different levels between different layers, which exploits local characteristics of ECG to characterize the spatial information representation. Then all the lead features are fused together as global features. To evaluate the generalization of proposed method and clinical utility, two schemes including the intra-patient scheme and inter-patient scheme are all employed.

Results: Experimental results based on PTB (Physikalisch-Technische Bundesanstalt) database shows that our model achieves superior results with the accuracy of 95.49%, the sensitivity of 94.85%, the specificity of 97.37%, and the F1 score of 96.92% for MI detection under the inter-patient scheme compared to the state-of-the-art. By contrast, the accuracy is 99.92% and the F1 score is 99.94% based on 5-fold cross validation under the intra-patient scheme. As for five types of MI location, the proposed method also yields an average accuracy of 99.72% and F1 of 99.67% in the intra-patient scheme.

* Corresponding author.

E-mail address: zzushi@126.com

Conclusions: The proposed method for MI detection and location has achieved superior results compared to other detection methods**.** However, further promotion of the performance based on MI location for the inter-patient scheme still depends significantly on the mass data and the novel model which reflects spatial location information of different leads subtly.

Keyword: myocardial infarction; convolutional neural network; residual blocks; feature fusion; automated detection; inter-patient scheme

1. Introduction

The prevalence of myocardial infarction (MI) is gradually increasing on account of overwork, excessive drinking and smoking, which caused myocardial necrosis by acute and sustained ischemia and hypoxia of coronary artery, leading permanent damage of heart muscle. Therefore, early detection and prevention of myocardial infarction are of great significance, which can ensure the life safety of patients[1]. Electrocardiogram (ECG) is the most commonly detection tools because of its convenience, noninvasiveness and low price, which shows the location and development period of pathological myocardium by the morphology of ST segment, T wave and QRS wave. Thus, it is spontaneous to detect MI using 12 leads ECG with artificial intelligence method.

Different methods to detect and locate MI have been widely employed. Most of the literatures were based on the procedure including the feature extraction, feature dimensionality and classification. Further, time domain analysis[2-4], frequency domain analysis[5-9], entropy[10-15], optimization algorithm[16, 17] are employed to extract the representative features. Principal component analysis is the most commonly dimensionality method among these papers. K Nearest Neighbors (KNN)[2, 10, 13], support vector machine (SVM)[4, 8, 12, 14, 16, 18], Decision Tree (DT)[19], Naive Bayes (NB)[20], Back Propagation neural network (BPNN)[3, 17] and other machine learning (ML) techniques have been widely adopted as the classification methods. In the past few years, deep learning (DL) methods, including convolutional neural networks (CNN), recurrent neural networks (RNN), restricted boltzman machines (RBM) and autoencoder (AE), are applied to the health care

domain based on physiological signals, such as ECG, EEG.[21, 22]. Acharya et al. [23, 24] proposed an end-to-end CNN structure using lead II ECG and signal lead including all 12 leads ECG signals, respectively. The model achieved better average performances with accuracy of 95.22% and 99.00%. Furthermore, Liu et al. [25, 26] designed an 2-D CNN structure and multiple feature branch CNN to detect MI, respectively. Moreover, Reasat et al. [27] presented a shallow CNN based on inception frame to detect inferior MI with lead II, III, and aVF, yielding the average performance of 84.54% accuracy. Meanwhile, LSTM method is also used to detect MI [28]. Besides, Lui et al. [29] employed a novel method that combined both CNN and RNN to classify MI based on a single lead ECG with the F1 score of 94.6%. In general, it is obvious that, CNN is the most widely utilized and achieves the best performance compared to all the methods. Hannun et al. [30] displayed 34 layers CNN structure consisting of 16 residual blocks with two convolutional layers per block to detect arrhythmia and exceeded the level of average cardiologists, showing the strongly perceptive ability of model.

While there are plenty of investigators on this issue of MI detection, many detailed questions are still unconsidered as follows. Firstly, CNN models, integrated feature extraction and classifier together, can automatically explore the representations from the raw ECG signal. However, the performance of basic CNN model is still to be further promoted based on feature fusion of different levels. Secondly, all the 12 leads ECG should be considered together which is coincident with the diagnostic rules of ECG towards MI, but many researchers only utilized the single lead ECG record or ECG beats, not 12 leads ECG records. Thirdly, few authors take the inter-patient scheme into account, which is closely related with the clinical practice due to considering individual differences along with different patients. Most papers only explored the intra-patient performance on standard ECG dataset, which cannot verify the effectiveness of the proposed model and lead to excessive optimistic results. Finally, the location of MI has great and constructive importance for clinician. Therefore, the overall performance of MI location needs to be enhanced.

Thus, in this paper, a novel Multi-Lead ResNet (ML–ResNet) based on residual

blocks and multi-lead feature fusion is proposed for MI detection. Compared to conventional ML methods and basic CNN model, ML–ResNet avoided to choose manual features and provided strong abilities of feature extraction and descriptor with residual blocks. More precisely, the main innovations are as follows:

- A novel ML–ResNet model combining a single lead feature branch network with three residual blocks and feature fusion method is employed to detect and locate MI via 12 leads ECG records.
- The single lead feature branch network can learn the representative features of different levels between different layers, which exploits local characteristics of ECG to characterize the spatial information representation.
- Two schemes including intra-patient scheme and inter-patient scheme, are both performed, displaying more vital clinical significance.
- Compared with published literatures, the proposed model for MI detection and location has achieved the best results.

The paper is organized as follows: section 2 presents the dataset and the pre-processing, the proposed algorithm is reported in section 3, section 4 shows the relevant results for MI detection and location under two schemes, the discussions and conclusions are introduced in section 5 and section 6, respectively.

2. Dateset and pre-processing

The database was from the PTB (Physikalisch-Technische Bundesanstalt). The PTB database contains of 15 simultaneously recorded signals including the conventional 12 leads ECG and the 3 Frank signals has been annotated by professional cardiologists, which is digitized at 1000Hz, with 16 bit resolution over a range of ±16.384 mV [31]. Generally, it can be observed from Table 1, that there are 312 MI recordings and 80 healthy control (HC) recordings from 113 MI patients and 52 HC patients. More precisely, there are 10 types of MI in the PTB database, and only five categories are selected to research the subject of MI location. All in all, 312 MI recordings consists of 47 anterior myocardial infarction recordings (AMI), 77 anteroseptal myocardial infarction recordings (ASMI), 43 anterolateral myocardial

infarction recordings (ALMI), 89 inferior myocardial infarction recordings (IMI), and 56 inferolateral myocardial infarction recordings (ILMI).

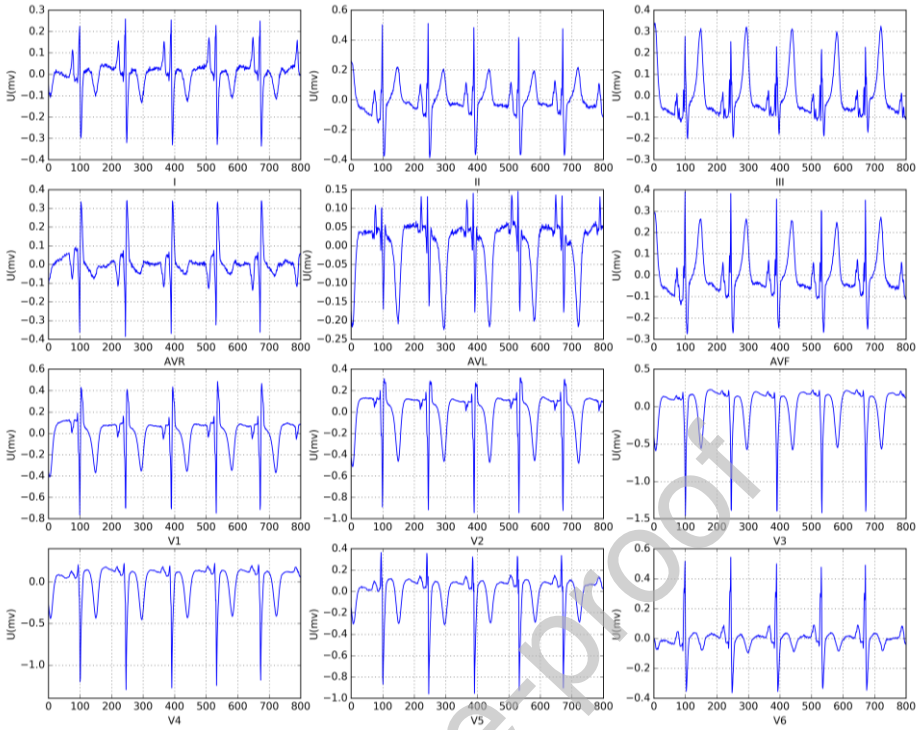

Figure 1. 12 leads ECG records after pre-processing

Table 1: Summary of PTB dataset samples in the paper

Class	No. of subjects	No. of records	No. of 12-lead records
HC	52	80	6945
MI	113	312	17212
AMI	17	47	2287
ASMI	27	77	4312
ALMI	16	43	2575
IMI	30	89	4452
ILMI	23	56	3586
Total	**165**	**392**	**24157**

HC：healthy control, MI：myocardial infarction, AMI: anterior myocardial infarction, ASMI: anteroseptal myocardial infarction recordings, ALMI: anterolateral myocardial infarction recordings, IMI: inferior myocardial infarction recordings, ILMI: inferolateral myocardial infarction recordings

The pre-processing steps include denoising, down-sampling, QRS detection and data augmentation. Wavelet denoising method is presented to eliminate different noise in the first step [32]. Then, the denoised signal is down sampled to 200Hz. Further, the Pan-Tompkins algorithm is employed to detect the QRS wave [33]. The method of

beat segmentation will be explored based on QRS detection. Concretely, 800 sample points will be chosen along with 99 points before QRS detection point and 700 points after QRS detection point. Finally, the number of PTB database can be increased based upon moving R-peak peak points. From Table 1, it is obvious there are 17212 MI recordings and 6945 HC recordings. Meanwhile, the number of five categories with MI is also added. Meanwhile, the myocardial infarction record is shown via pre-processing in Figure 1.

3. Methods

The proposed ML-ResNet network is employed to detect MI and localize MI, which has 13 layers including one lead feature branch. In detail, the single feature branch consists of 3 residual blocks with three convolutional layers per block. Fig. 2 displays a graphical representation of the architecture of the model.

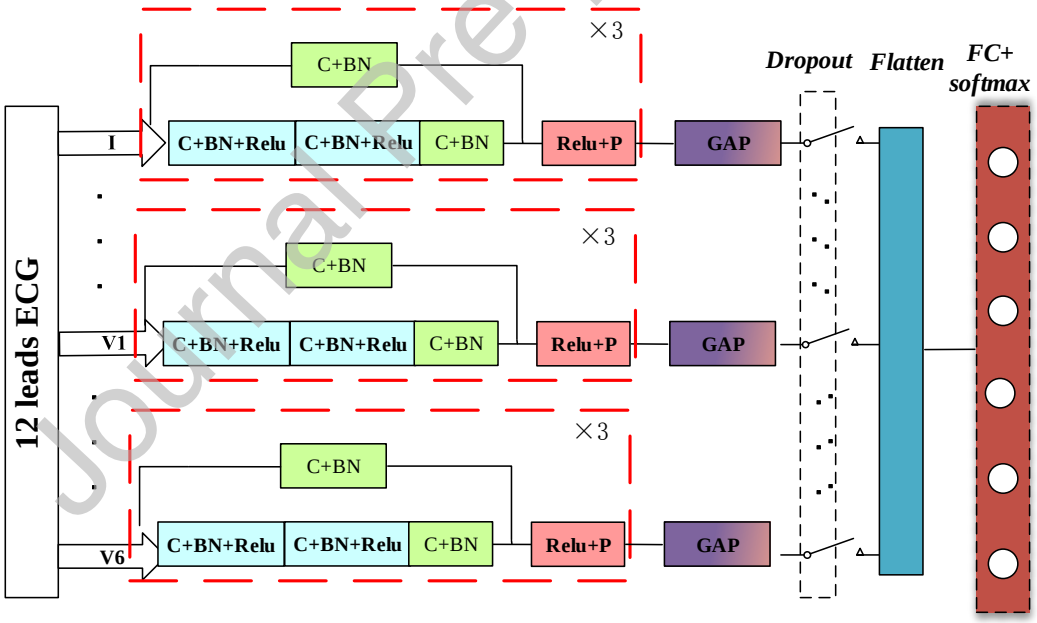

Figure 2. The architecture of the proposed ML–ResNet

3.1. Single lead feature branch network

Deep residual network (ResNet) is firstly developed to improve the performance of image classification based on ImageNet database by Kaiming He in 2016 [34]. With the layers of deep network are increasing, the model still maintain a strong

ability by solving the problems of vanishing and exploding gradients along with degradation by the concept of identify mapping. Meanwhile, true integration of different levels of features between different layers are utilized to extract strong correlation representational features. Considering that ECG signals between different leads are independent, commonly used convolutional networks, namely using the same kernel between different leads, is not suitable for MI detection and location based on 12 leads ECG records.

Hence, single lead feature branch network for every lead should be introduced, which consists of residual blocks, including convolutional layer (C), batch normalization layer (BN), rectified linear unit layer (Relu), and pooling layer (P). The convolutional layer [35] is utilized to capture remarkable features, which has the characteristic of translation invariance, size invariance and rotation invariance; the distribution of the feature map based on the convolutional layer changes in the processing of forward propagation and back propagation all the time, the following layers named batch normalization layer play a role in normalization towards the output, which can keep the stability of gradient size to continuously adopt to new change [36]. The Relu layer has an important effect on improving the performance of CNN model based on a nonlinearity transform. The Relu operation can be overviewed with the equation: $f(x) = \max(x; 0)$, which introduces the sparsity and alleviates the occurrence of over fitting by reducing the inter-dependence of parameters [37]. Going further, pooling layer including average pooling layer and global average pooling layer (GAP) [38], which reduces feature dimension and provides more specific internal representation. Above all, GAP which gives the actual category meaning of each channel, as a method of feature selection, can effectively prevent over fitting by regularization without learning any parameters. In fact, GAP layer and dropout layer can all reduce over fitting. Of course, I did the experiment to display the performance without using dropout layer. The results show that the performance is much the same regardless of whether this method is used or not, sometimes it is slightly less than 0.1 percent without the dropout layer.

Table 2 summarizes the architecture of three residual blocks of the model. Every residual block network includes three convolutional layers, whose layer are followed by a Relu operation and batch normalization operation, and an average pooling layer. An additional convolutional layer with a 1×1 filter and batch normalization layer are developed to increase the dimension to be used for addition in the residual block. As each residual block is designed to learn fused ECG features at multiple spatial resolution, the filter shape with N filters is M×1 in the convolutional layer. M began with 17 and was reduced to 5 after the third layer, while N began with 2 and was added to 4 in the second layer and to 8 in the third layer. Meanwhile, the input used the mode of zero padded to keep the output length immobile. The operation of residual blocks can be formulated as:

$$y_i = \mathrm{P}\{\mathrm{relu}[x_i + E(x_i)] + F(x_i, w_i)\} \quad (1)$$

Where x_i and y_i are the i-th input and output of residual block; W_i is the 1-D convolutional kernel (or weight); $E(x_i)$ represents the dimension transformation to satisfy the operation of add; $F(x_i, w_i)$ denotes multiple the 1-D convolution operation connecting batch normalization and Relu layer. A new convolutional layer and batch normalization layer are connected to the three residual blocks to further extract the useful information. In addition, GAP and dropout with a probability of 0.5 is also applied to extract core features and promote generalization ability.

Table 2: Architecture of three residual blocks of the model

Type	Kernel/Pool size	Number of kernel
input	-	-
Convolutional 1D	17×1	2/4/8
BN+Relu	-	-
Convolutional 1D	11×1	2/4/8
BN+Relu	-	-
Convolutional 1D	5×1	2/4/8
BN	-	-
Expand input (C)	1×1	2/4/8
Skip connection	-	-
Pooling	5	-

3.2 Multi-lead feature fusion

12 leads feature can be extracted by single lead feature branch network. Then all the 12 leads features are combined, the representative feature vector D can be acquired,

$$D=[D_1,D_2,D_3,D_4,D_5,D_6,D_7,D_8,D_9,D_{10},D_{11},D_{12}] \quad (2)$$

Where its dimensionality is 16×12. Flatten layer can reshape the dimensionality from 16×12 to 192×1. After this layer, the data are fed to the output layer using the softmax function. Meanwhile, the final fully connected softmax layer produces a distribution over the 2 output classes or 6 classes for MI detection and MI location, respectively. Detailed information of ML–ResNet is listed in Table 3.

Table 3: Detailed information of ML–ResNet

Layers	Type	Number of kernel	Output shape
0	Input	-	800×1
1-4	Residual block	2	160×2
5-8	Residual block	4	32×4
9-12	Residual block	8	6×8
-	GAP	-	1×8
-	Dropout	-	1×8
-	Flatten		12×8
13	Fully-connected		**2 or 6**

3.3 Training

The ML–ResNet model was trained incorporating the loss function of categorical cross entropy and the stochastic gradient descent (SGD) optimizer with the momentum of 0.9 and learning rate of 0.001 [39]. Training would be stopped if there was no improvement in the processing of training for 10 consecutive epochs. The training was allowed to run for a maximum of 60 epochs along with a mini batch size of 512. Moreover, the model that achieved the lowest error on the testing dataset are chosen. Hyper-parameters including learning rate, mini batch size, and the number of epochs seriously effects the overall performance of MI detection and location, which are selected tuned by trial and error.

3.4 Performance evaluation

Different medical clinical indicators along with sensitivity (Se), specificity (Sp), positive predictive value (PPV), accuracy (Acc) and F-measure (F1) are used for MI detection and location. They are defined as follows:

$$Se = \frac{TP}{TP + FN} \times 100\% \tag{3}$$

$$Sp = \frac{TN}{TN + FP} \times 100\% \tag{4}$$

$$PPV = \frac{TP}{TP + FP} \times 100\% \tag{5}$$

$$Acc = \frac{TP + TN}{TP + TN + FP + FN} \times 100\% \tag{6}$$

$$F1 = 2 \cdot \frac{Se \cdot PPV}{Se + PPV} \times 100 \tag{7}$$

Where TP and TN represent the number of true positive and true negative patients, respectively. FN and FP indicate the quantity of false negative and false positive, which mean that MI is regarded as the HC and HC is misclassified MI, respectively.

4. Results

4.1 Experimental settings

Experimental studies for MI detection and MI location under intra-patient scheme and inter-patient scheme in the PTB dataset are implemented with the same deep model. Without changing any parameters of the ML-ResNet model, only the distribution of dataset is changed to satisfy the mode of inter-patient. The experiments about MI detection and location are discussed and conducted on python package with Keras [40], along with the hardware configuration of Intel Xeon(R) E3-1225 GPU 8 GHz and NVIDIA Geforce GTX 1070 of GPU. This server runs a windows 10 system, and these experiment can be finished about 12 s to 14 s every epoch.

4.2 Results of MI detection and location under intra-patient scheme

The performance of MI detection along with MI location is analyzed based upon 5-fold cross validation in this part. Specifically, 24157 records including HC and various MI are divided into 5 equal parts, which have the same number between the two classes for MI detection and six classes for MI location. A total of 19326 MI and HC records are employed in the training phase. Oppositely, a sum of 4831 records are used in the testing phase. As a result, all the 24157 records will be exploited based on cross validation.

Table 4: 5-fold cross validation results of MI detection based on intra-patient scheme

Fold	Acc(%)	Se(%)	Sp(%)	PPV(%)	F1(%)
1	**99.92**	**99.88**	**100.00**	**100.00**	**99.94**
2	**99.86**	**100.00**	**99.50**	**99.80**	**99.90**
3	**100.00**	**100.00**	**100.00**	**100.00**	**100.00**
4	**100.00**	**100.00**	**100.00**	**100.00**	**100.00**
5	**99.81**	**100.00**	**99.36**	**99.74**	**99.87**
Average	**99.92**	**99.98**	**99.77**	**99.91**	**99.94**

Table 5: Confusion matrix and performance for MI detection across 5-fold cross validation based on intra-patient scheme

		Predicted		Acc(%)	Se(%)	Sp(%)	PPV (%)	F1(%)
		MI	HC					
Original	MI	17208	4	**99.92**	**99.98**	**99.77**	**99.91**	**99.94**
	HC	16	6929					

By combining the results in Tables 4 and 5, it is obvious that our algorithm along with ML-ResNet model achieves a good overall performance based upon MI detection. The overall performance including accuracy, sensitivity, specificity, PPV along with F1 are 99.92%, 99.98%, 99.77%, 99.91% and 99.94% in Table 4, respectively. As for the fifth fold in the experiment, only 0.19% of the ECG records are incorrectly identified, which displays the superiority of the proposed model. Meanwhile, all the MI and HC records are fully detected with F1 of 100% in the third and fourth fold. Moreover, the algorithm is reliable enough. The difference of

different folds is slight, displaying the strong robustness. It is obvious from Table 5, that only 4 MI records and 16 HC records are misclassified. Furthermore, 17208 MI records out of 17212 records are correct detected, which indicate the false negative rate is very low. Meanwhile, the area under the curve (AUC) which is calculated by receiver operating characteristic curve is present to show the performance for MI detection in Figure 3, which indicats the AUC for intra-patient scheme is 1.00, in fact it is 0.9999.

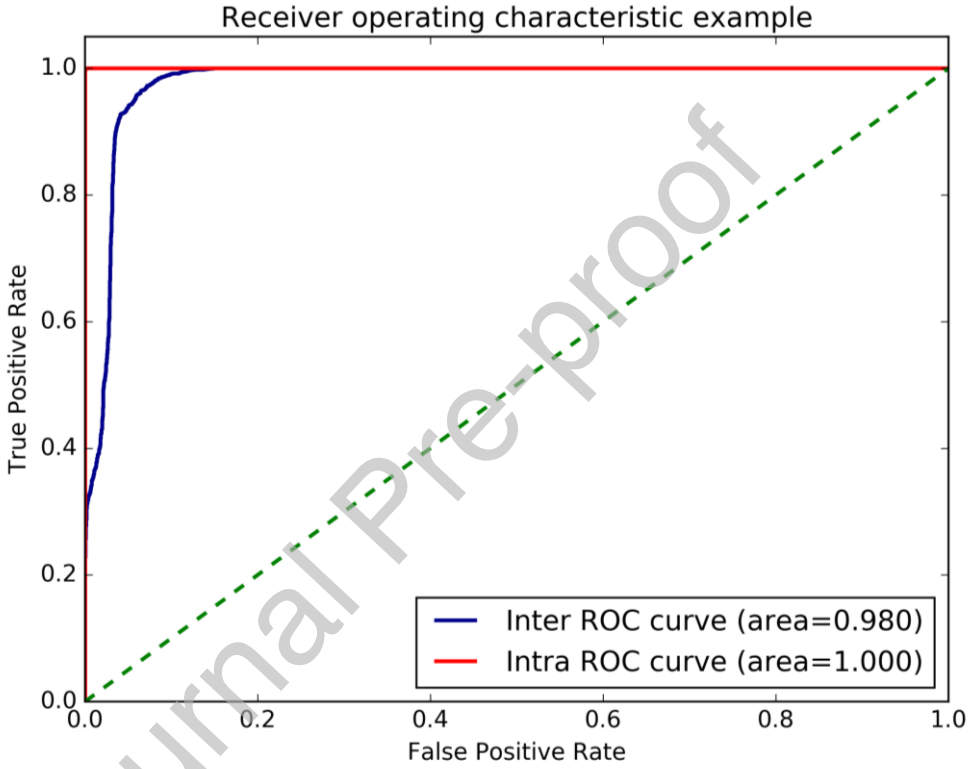

Figure 3. ROC curves of the proposed method about MI detection based on two schemes

Table 6: 5-fold cross validation results of MI location based on intra-patient scheme

Fold	Acc(%)	Se (%)	Sp(%)	PPV(%)	F1(%)
1	99.61	99.47	99.60	99.56	99.51
2	99.73	99.68	99.73	99.68	99.68
3	99.81	99.78	99.81	99.78	99.78
4	99.81	99.75	99.81	99.81	99.78
5	99.63	99.46	99.62	99.63	99.54
Average	99.72	99.63	99.72	99.69	99.67

Table 7: Confusion matrix and performance for MI location across 5-fold cross validation based on intra-patient scheme

	Predicted						Acc(%)	Se(%)	Sp(%)	PPV(%)	F1(%)
	AMI	ASMI	ALMI	IMI	ILMI	HC					
AMI	2262	17	3	0	0	0	99.72	99.12	99.78	99.87	99.49
ASMI	2	4323	8	1	2	0	99.72	99.70	99.72	99.27	99.48
ALMI	1	14	2560	0	1	0	99.72	99.38	99.76	99.57	99.48
IMI	0	1	0	4441	12	1	99.72	99.69	99.73	99.89	99.79
ILMI	0	0	0	4	3578	0	99.72	99.89	99.69	99.56	99.72
HC	0	0	0	0	1	6926	99.72	99.99	99.61	99.99	99.99
AVE	/	/	/	/	/	/	99.72	99.63	99.72	99.69	99.67

In fact, MI location is complex than MI detection, which show the dynamic ECG change in different leads. As illustrated in Table 6, the ML-ResNet model correctly recognizes the data in the AMI, ASMI, ALMI, IML, ILMI, HC classes, which achieves the excellent average performance across 5 folds. Specifically, the accuracy, sensitivity, specificity, along with F1 respectively are 99.72%, 99.63%, 99.72% and 99.67%. Confusion matrix and performance for MI location across 5-fold cross validation based on intra-patient scheme are given in Table 7. It is easy to discover that 17 AMI records are regarded as ASMI, and 14 ALMI records are considered as ASMI. In fact, all the above-mentioned records all belong to the anterior MI, therefore it is hard to distinguish these categories. It is evidence that from figure1 almost no IMI records are detected as AMI records or HC records, showing the excellent performance of the proposed model. From Figure 4 and figure 5, it is obvious that the loss curve and accuracy are steadily decreasing and increasing and display excellent results under intra-patient schemes for MI detection and MI location, respectively.

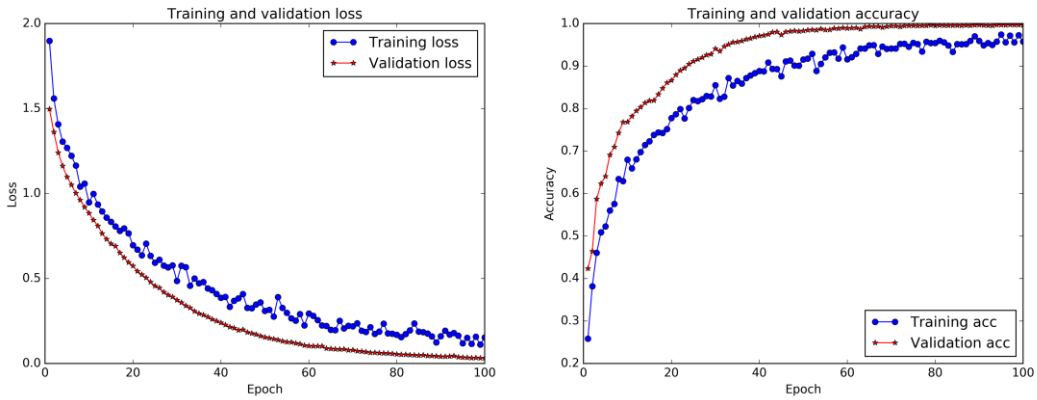

Figure 4. Training (blue lines) and validating (red lines) performance graphs based on MI detection under intra-patient scheme
a) Loss curve(at left) and b) accuracy (at right).

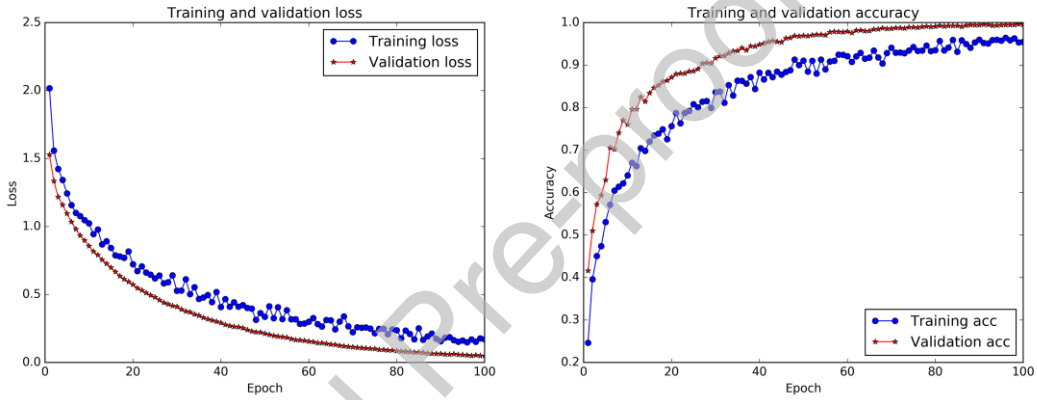

Figure 5. Training (blue lines) and validating (red lines) performance graphs based on MI location under intra-patient scheme
a) Loss curve(at left) and b) accuracy (at right).

4.3 Results of MI detection and location under inter-patient scheme

Different from aforementioned intra-patient experiments, the inter-patient scheme has an important clinical significance to prove the generalization of the model. For the PTB database, 55 HC patients and 209 MI patients are employed in the training stage, meanwhile the remaining 25 HC patients and 103 MI patients are employed in the testing stage. In total, 4740 HC and 10721 MI 12 leads ECG records are utilized to train the model, and the rest of 2205 HC records and 6491 MI records are utilized to analyze the performance under the inter-patient scheme after the procedure of pre-processing. By analyzing the results in Tables 8 and 9, it is apparent that the overall performance under the inter-patient scheme is worse compared to the intra-patient scheme in Tables 6 and 7.

From Table 8, that out of a total of 6491 MI records only 6157 records are detected, which indicates the average performance of 95.49% accuracy, 94.85% sensitivity, 97.37% specificity, 99.07% PPV and 96.92% F1. The Se and Sp for MI detection is 94.85% and 97.37%. The results show that the probability of correct detection of HC records from ECG signals is higher than that of MI records. Meanwhile, Figure 6 presents the results of training (blue lines) and testing (red lines) performance based on loss curve and accuracy curve during 60 epochs, which also shows the convergence of the proposed algorithm is better and don't occur the phenomenon of over fitting. Furthermore, Figure 3 displays that the AUC is 0.98 based on the inter-patient scheme.

Table 8: Confusion matrix for MI detection based on inter-patient scheme

		Predicted		Acc(%)	Se(%)	Sp(%)	PPV(%)	F1(%)
		MI	HC					
Original	MI	6157	334	**95.49**	**94.85**	**97.37**	**99.07**	**96.92**
	HC	58	2147					

Table 9: Confusion matrix for MI location based on inter-patient scheme

	Predicted						Acc(%)	Se(%)	Sp(%)	PPV(%)	F1(%)
	AMI	ASMI	ALMI	IMI	ILMI	HC					
AMI	251	93	23	0	5	401	55.74	32.47	58.01	54.45	40.68
ASMI	57	1295	29	166	124	153	55.74	71.00	51.688	70.92	70.96
ALMI	90	357	235	37	180	52	55.74	24.71	59.55	78.60	37.60
IMI	0	78	12	607	480	495	55.74	36.30	60.36	48.44	41.50
ILMI	63	2	0	414	284	508	55.74	22.35	61.46	26.47	24.23
HC	0	1	0	29	0	2175	55.74	98.64	41.17	57.48	72.63
AVE	/	/	/	/	/	/	55.74	47.58	55.37	56.06	47.94

At first glimpse of Table 9, it can be concluded that the accuracy and other performance criterion for MI location are all low compared to all the experiments above. In detail, the best result is that the sensitivity of HC class is 98.64%, showing most HC records are correctly detected. Many MI records are wrongly classified as HC on account of intrinsic imbalanced distribution about the subject between MI and HC in Table 1. As shown in Figure 7, the loss curve and accuracy are steadily decreasing and increasing, respectively. However, the over performance can not be promoted in the earlier epochs. The results are consistent with the number of patient in the dataset even although oversampling has been applied in the stage of pre-processing.

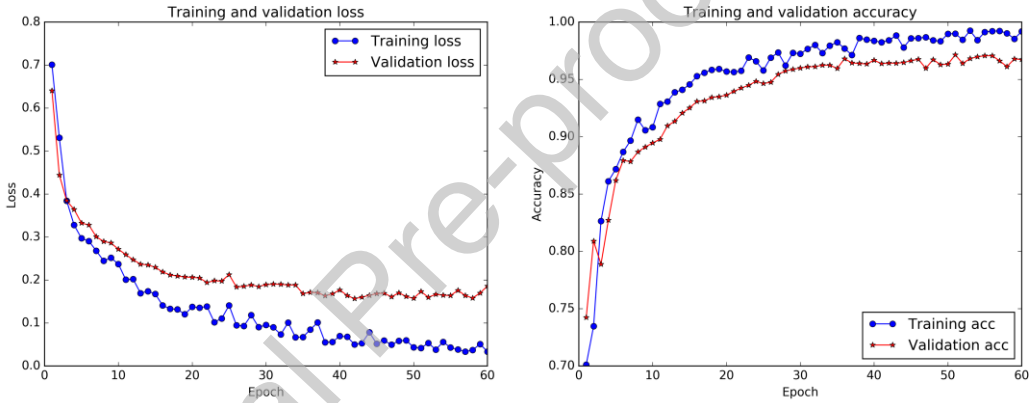

Figure 6. Training (blue lines) and validating (red lines) performance graphs based on MI detection under inter-patient scheme
a) Loss curve(at left) and b) accuracy (at right).

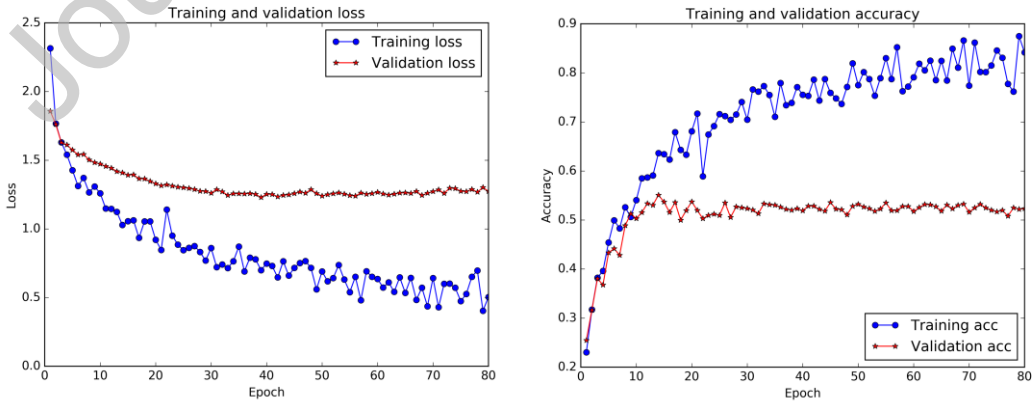

Figure 7. Training (blue lines) and validating (red lines) performance graphs based on MI location under inter-patient scheme
a) Loss curve(at left) and b) accuracy (at right).

4.4 Compared with other models

To verify the validity of the model, the basic CNN (BCNN) and the LSTM module compared with the ML-ResNet model and GAP layer for MI detection based on the inter-patient scheme in the proposed model are displayed. BCNN is the base model which has the same parameters and lacks of residual blocks with ML-ResNet. Meanwhile, it can be utilized to display the effectiveness of residual block. The average performance among these control groups are listed in Table 10. According to the comparison, it is obvious that the proposed ML-ResNet has more excellent performance than BCNN and ML-ResNet using GAP layer, which shows the availability of employing residual blocks and GAP layer about the model. Generally, the residual blocks in the model can learn more fused and effective features from different layers and facilitate the traing mode by comparison with the basic CNN. Additionally, the GAP layer can extract these focused features output by the previous CNN layer with more space information, which has the better ability to select the optimal features than LSTM. After all, LSTM layer pays attention to the correlation of time series. Finally, 12 leads feature fusion from every single lead feature branch network based on 12 leads ECG records is accordant with the clinical diagnostic criteria.

Table 10: The comparison results among different models

Model	module	Acc(%)	Se(%)	Sp(%)	PPV(%)	F1(%)
ML-BCNN	-	93.80	82.04	99.00	90.24	92.35
ML-ResNet	LSTM	93.41	91.71	94.47	88.73	90.54
	GAP	**95.49**	**94.85**	**97.37**	**99.07**	**96.92**

5. Discussions

There are many approaches for MI detection and MI location based on ECG records in the literature. Almost all the researchers employ the PTB database with different numbers by pre-processing. Different classification patterns and the number of lead and MI classes with proposed model using ML and DL methods, should be

noted when comparing the corresponding performances. Table 11 presents a comparison of the results of some recent studies and the current proposed model for MI detection and MI location.

MI detection were all evaluated by similar method based on different entropies along with time-frequency transform and shallow classifiers under intra-patient schemes, which achieved higher performance[10, 12, 15]. Among these studies, two studies leveraged the pattern of intra-patient for MI detection, it is obvious that accuracy, sensitivity and specificity need to be improved[12, 15]. Five out of eight comparison articles in Table 11 used the end-to-end CNN structure to detect and locate MI. Reasat et al. [27] and Liu et al. [25] only occupied three and four leads for MI detection, achieving generalized results under intra-patient schemes and inter-patient schemes. Baloglu et al. [24] yielded impressive results based on CNN model with every lead. Actually, 12 leads ECG is very important to distinguish MI and HC records. The specific ECG leads with relevant QRS, ST segment and T wave morphology will exhibit the change to display the area of MI. For example, ECG wave of IMI patients makes a difference among II, III and AVF leads. Analogously, the morphology of QRS wave, T wave and ST segment will change for AMI patients. Liu et al. [26, 28] used multiple feature-branch CNN model and CNN along with BLSTM model using 12 leads ECG records, respectively. The models can capture temporal properties using BLSTM by 12 leads and obtain good results, however further exploration about MI location on two classification pattern has not been done. Notably, the performance of MI detection in view of inter-patient pattern is still to be promoted. Moreover, different leads represented the spatial position of the heart, whose information should be focused on spatial information representation, not the temporal information. Hence, automated MI detection and localization model based on two schemes using 12 ECG leads records, namely, ML-ResNet network, is proposed, which can effectively help clinicians to detect MI and confirm the location of infarcted myocardium, providing auxiliary diagnostic as a tool. Although the model shows a bad performance for MI location for inter-patient pattern, it is limited by the

number of MI patient of PTB database. Going further, the weakness of proposed model is lack of interpretability, which is also the drawbacks of DL. More excellent methods or models combined with clinical knowledge should be researched about this theme.

Finally, this is the first paper to research MI location with 12 leads ECG records for inter-patient schemes. Though the performance is poor for MI location for inter-patient schemes, it is very meaningful to explore it. More valuable questions need to be studied. After all, the number of different MI is very small as shown in Table 1. Data augmentation cannot make up the individual differences among patients. More patient data is necessary to improve the performance for MI location based on inter-patient schemes. Aiming at the problem of selecting the leads of ECG, the results are labeled based on 12 leads ECG records for the PTB database. If one lead or multiple lead are employed, the label will be wrong. Maybe the selected leads do not contain the changes of QRS, ST segment and T wave morphology.

Table 11: Comparison of the proposed method and results for MI detection and location on ECG

Study	Datasets	Methods	MI detection	MI location	Scheme	
					Intra	Inter
[10] 2016	3 leads 485753 MI, 125652 Normal	DWT approximate entropy, fuzzy entropy, permutation entropy, etc; KNN SWT	Yes	Yes	Detection: Acc = 98.8% Se= 99.45% Location: Acc=98.74% Se= 99.55%	No
[15] 2017	3 leads 3240 IMI , 3037Normal	Sample entropy, log energy entropy, and median slope; KNN/SVM	Yes	No	Acc=98.84% Se= 99.35% Sp= 98.29%	Acc=81.71% Se=79.01% Sp= 79.26%
[27] 2017	3 leads 3222 IMI , 3055Normals	Shallow CNN with inception network	Yes	No	No	Acc=84.54% Se=85.33% Sp=84.09%
[23] 2017	1 lead 485752 MI, 125652 Normal	Deep CNN	No	Yes	Acc=99.78%	No
[25]	4 leads	Multilead-	Yes	No	Detection:	No

2018	167 MI, 80 Normal	2DCNN			Acc=96.00% Se=95.40% Sp=97.37%	
[26] 2018	12 leads 48690 MI, 10646 normal	Multiple feature-branch CNN	Yes	Yes	Detection: Acc=99.95% Se= 99.97% Sp= 99.90% Location: Acc=99.81%	No
[12] 2019	12 leads 28213MI, 5373Normal	energy entropy based on MODWPT; morphological features; SVM	Yes	No	Acc=99.75% Se= 99.37% ppv=99.70%	Acc=92.69% Se=80.96% ppv=86.14%
[28] 2019	12 leads 53712 MI, 10638 normal	CNN+BLSTM	Yes	No	Acc=99.90% Se= 99.97% Sp= 99.54%	Acc=93.08% Se= 94.42% Sp= 86.29%
Prop osed	12 leads 28213MI , 5373Normal	ML-ResNet	Yes	Yes	Detection: Acc=99.92% Se= 99.98% Sp= 99.77% F1=99.94% Location: Acc=99.72% Se= 99.63% Sp= 99.72% F1=99.67%	Detection: Acc=95.49% Se= 94.85% Sp=97.37% F1=96.92% Location: Acc=55.74% Se=47.58% Sp=55.37% F1=47.94%

Acc: Accuracy, Se: Sensitivity, Sp: Specificity, SWT: Stationary Wavelet Transform, DWT: Discrete Wavelet Transform, BLSTM: Bidirectional Long Short Term Memory; MODWPT: maximal overlap discrete wavelet packet transform

6. Conclusions

In this paper, a novel ML-ResNet model for the detection and localization of MI is present, by using residual blocks to fuse the representational features of different levels between different layers and multiple feature combination method from 12 leads ECG records. A total of four experiments, integrating two classification pattern with MI detection and MI location, are conducted and verified based on PTB diagnostic ECG database. Meanwhile, BCNN model and the LSTM module compared with the ML-ResNet model and GAP layer for MI detection are also described.

From the results, the proposed method can availably detect and locate MI based on 12 leads ECG records with excellent classification performances under intra-patient scheme and inter-patient scheme in Table 10. Moreover, ML-ResNet model performs better than other contrastive models. Specifically, the average results of our method **are** accuracy of 99.92%, F1 of 99.94% based on 5-fold cross validation for intra-patient scheme and accuracy of 95.49%, F1 of 96.92% for inter-patient scheme. Once again, the performance of MI location consisting of 5 types of MIs and HC for two classification patterns is also presented. The model yields accuracy, sensitivity and specificity over 99.50% on intra-patient scheme. Limited by the number of MI patient of PTB database, the overall performance to locate MI on inter-patient scheme is not good.

In future, more representational features using ECG that can explain the reason of availability should be employed under the inter-patient scheme, such as vectorcardiogram indicating the information about direction and speed. Above all, high quality ECG datasets with labels are the most crucial to promote the overall performance of ECG intelligent diagnosis. The novel model with high performance has the potential to run on wearable ECG devices in the family and monitoring equipment in the hospital, which is coincident with the doctor's diagnosis logic along with 12 leads ECG. Furthermore, these methods can save the patient's life and reduce workload for doctors working in ECG department.

Acknowledgement

This research is funded by Key Laboratory of Intelligence Technology and System, in Beijing National Research Center for Information Science and Technology.

Conflict of interests

The authors declare that they have no known competing financial interests or personal relationships that could have appeared to influence the work reported in this paper.

Reference

[1] K. Thygesen, J.S. Alpert, A.S. Jaffe, B.R. Chaitman, J.J. Bax, D.A. Morrow, H.D. White, E.S.C.S.D. Group, Fourth universal definition of myocardial infarction (2018), European heart journal, 40 (2019) 237-269.

[2] M. Arif, I.A. Malagore, F.A. Afsar, Detection and Localization of Myocardial Infarction using K-nearest Neighbor Classifier, Journal of Medical Systems, 36 (2010) 279-289.

[3] R.S. Remya, K.P. Indiradevi, K.K.A. Babu, Classification of Myocardial Infarction Using Multi Resolution Wavelet Analysis of ECG, Procedia Technology, 24 (2016) 949-956.

[4] A.K. Dohare, V. Kumar, R. Kumar, Detection of myocardial infarction in 12 lead ECG using support vector machine, Applied Soft Computing, 64 (2018) 138-147.

[5] A. Diker, Z. Comert, E. Avci, S. Velappan, Intelligent system based on Genetic Algorithm and support vector machine for detection of myocardial infarction from ECG signals, 2018 26th Signal Processing and Communications Applications Conference (SIU), (2018) 1-4.

[6] S. Banerjee, M. Mitra, Application of Cross Wavelet Transform for ECG Pattern Analysis and Classification, IEEE Transactions on Instrumentation and Measurement, 63 (2014) 326-333.

[7] U.R. Acharya, H. Fujita, M. Adam, O.S. Lih, V.K. Sudarshan, T.J. Hong, J.E.W. Koh, Y. Hagiwara, C.K. Chua, C.K. Poo, T.R. San, Automated characterization and classification of coronary artery disease and myocardial infarction by decomposition of ECG signals: A comparative study, Information Sciences, 377 (2017) 17-29.

[8] L.N. Sharma, R.K. Tripathy, S. Dandapat, Multiscale Energy and Eigenspace Approach to Detection and Localization of Myocardial Infarction, IEEE transactions on bio-medical engineering, 62 (2015) 1827-1837.

[9] D. Sadhukhan, S. Pal, M. Mitra, Automated Identification of Myocardial Infarction Using Harmonic Phase Distribution Pattern of ECG Data, IEEE Transactions on Instrumentation and Measurement, 67 (2018) 2303-2313.

[10] U.R. Acharya, H. Fujita, V.K. Sudarshan, S.L. Oh, M. Adam, J.E.W. Koh, J.H. Tan, D.N. Ghista, R.J. Martis, C.K. Chua, C.K. Poo, R.S. Tan, Automated detection and localization of myocardial infarction using electrocardiogram: a comparative study of different leads, Knowledge-Based Systems, 99 (2016) 146-156.

[11] R.K. Tripathy, A. Bhattacharyya, R.B. Pachori, A Novel Approach for Detection of Myocardial Infarction from ECG Signals of Multiple Electrodes, IEEE Sensors Journal, (2019) 1-1.

[12] C. Han, L. Shi, Automated interpretable detection of myocardial infarction fusing energy entropy and morphological features, Computer Methods and Programs in Biomedicine, 175 (2019) 9-23.

[13] M. Sharma, R.S. Tan, U.R. Acharya, A novel automated diagnostic system for classification of myocardial infarction ECG signals using an optimal biorthogonal filter bank, Computers in Biology and Medicine, 102 (2018) 341-356.

[14] M. Kumar, R. Pachori, U. Acharya, Automated Diagnosis of Myocardial Infarction ECG Signals Using Sample Entropy in Flexible Analytic Wavelet Transform Framework, Entropy, 19 (2017) 488.

[15] L.D. Sharma, R.K. Sunkaria, Inferior myocardial infarction detection using stationary wavelet transform and machine learning approach, Signal, Image and Video Processing, 12 (2017) 199-206.

[16] P. Kora, S.R. Kalva, Improved Bat algorithm for the detection of myocardial infarction,

SpringerPlus, 4 (2015).
[17] P. Kora, ECG based Myocardial Infarction detection using Hybrid Firefly Algorithm, Computer Methods and Programs in Biomedicine, 152 (2017) 141-148.
[18] S. Padhy, S. Dandapat, Third-order tensor based analysis of multilead ECG for classification of myocardial infarction, Biomedical Signal Processing and Control, 31 (2017) 71-78.
[19] B. Liu, J. Liu, G. Wang, K. Huang, F. Li, Y. Zheng, Y. Luo, F. Zhou, A novel electrocardiogram parameterization algorithm and its application in myocardial infarction detection, Computers in Biology and Medicine, 61 (2015) 178-184.
[20] N. Safdarian, N.J. Dabanloo, G. Attarodi, A New Pattern Recognition Method for Detection and Localization of Myocardial Infarction Using T-Wave Integral and Total Integral as Extracted Features from One Cycle of ECG Signal, Journal of Biomedical Science and Engineering, 07 (2014) 818-824.
[21] R. Miotto, F. Wang, S. Wang, X. Jiang, J.T. Dudley, Deep learning for healthcare: review, opportunities and challenges, Briefings in Bioinformatics, 19 (2018) 1236-1246.
[22] O. Faust, Y. Hagiwara, T.J. Hong, O.S. Lih, U.R. Acharya, Deep learning for healthcare applications based on physiological signals: A review, Comput Methods Programs Biomed, 161 (2018) 1-13.
[23] U.R. Acharya, H. Fujita, S.L. Oh, Y. Hagiwara, J.H. Tan, M. Adam, Application of deep convolutional neural network for automated detection of myocardial infarction using ECG signals, Information Sciences, 415-416 (2017) 190-198.
[24] U.B. Baloglu, M. Talo, O. Yildirim, R.S. Tan, U.R. Acharya, Classification of myocardial infarction with multi-lead ECG signals and deep CNN, Pattern Recognition Letters, 122 (2019) 23-30.
[25] W. Liu, M. Zhang, Y. Zhang, Y. Liao, Q. Huang, S. Chang, H. Wang, J. He, Real-Time Multilead Convolutional Neural Network for Myocardial Infarction Detection, IEEE Journal of Biomedical and Health Informatics, 22 (2018) 1434-1444.
[26] W. Liu, Q. Huang, S. Chang, H. Wang, J. He, Multiple-feature-branch convolutional neural network for myocardial infarction diagnosis using electrocardiogram, Biomedical Signal Processing and Control, 45 (2018) 22-32.
[27] T. Reasat, C. Shahnaz, Detection of inferior myocardial infarction using shallow convolutional neural networks, 2017 IEEE Region 10 Humanitarian Technology Conference (R10-HTC), (2017) 718-721.
[28] W. Liu, F. Wang, Q. Huang, S. Chang, H. Wang, J. He, MFB-CBRNN: a hybrid network for MI detection using 12-lead ECGs, IEEE J Biomed Health Inform, (2019).
[29] H.W. Lui, K.L. Chow, Multiclass classification of myocardial infarction with convolutional and recurrent neural networks for portable ECG devices, Informatics in Medicine Unlocked, 13 (2018) 26-33.
[30] A.Y. Hannun, P. Rajpurkar, M. Haghpanahi, G.H. Tison, C. Bourn, M.P. Turakhia, A.Y. Ng, Cardiologist-level arrhythmia detection and classification in ambulatory electrocardiograms using a deep neural network, Nature medicine, 25 (2019) 65-69.
[31] A.L. Goldberger, L.A.N. Amaral, L. Glass, J.M. Hausdorff, P.C. Ivanov, R.G. Mark, J.E. Mietus, G.B. Moody, C.-K. Peng, H.E. Stanley, PhysioBank, PhysioToolkit, and PhysioNet, Circulation, 101 (2000).
[32] R.J. Martis, U.R. Acharya, L.C. Min, ECG beat classification using PCA, LDA, ICA and Discrete Wavelet Transform, Biomedical Signal Processing and Control, 8 (2013) 437-448.
[33] J. Pan, W.J. Tompkins, A real-time QRS detection algorithm, IEEE transactions on bio-medical

engineering, 32 (1985) 230-236.
[34] K. He, X. Zhang, S. Ren, J. Sun, Deep Residual Learning for Image Recognition, Computer Vision and Pattern Recognition, (2016) 770-778.
[35] A. Krizhevsky, I. Sutskever, G.E. Hinton, ImageNet Classification with Deep Convolutional Neural Networks, in: International Conference on Neural Information Processing Systems, 2012.
[36] S. Ioffe, C. Szegedy, Batch Normalization: Accelerating Deep Network Training by Reducing Internal Covariate Shift, (2015).
[37] V. Nair, G.E. Hinton, Rectified Linear Units Improve Restricted Boltzmann Machines, in: International Conference on International Conference on Machine Learning, 2010.
[38] M. Lin, Q. Chen, S. Yan, Network in network, arXiv preprint arXiv:1312.4400, (2013).
[39] Y. LeCun, Y. Bengio, G. Hinton, Deep learning, nature, 521 (2015) 436.
[40] A. Gulli, S. Pal, Deep Learning with Keras, Packt Publishing Ltd, 2017.